

Overview of the FTU Results

B. Angelini, S.V. Annibaldi, M.L. Apicella, G. Apruzzese, E. Barbato, A. Bertocchi, F. Bombarda, C. Bourdelle³, A. Bruschi¹, P. Buratti, G. Calabrò, A. Cardinali, L. Carraro², C. Castaldo, C. Centioli, R. Cesario, S. Cirant¹, V. Cocilovo, F. Crisanti, R. De Angelis, M. De Benedetti, F. De Marco, B. Esposito, D. Frigione, L. Gabellieri, F. Gandini¹, L. Garzotti², E. Giovannozzi, **C. Gormezano**, F. Gravanti, G. Granucci¹, G.T. Hoang³, F. Iannone, H. Kroegler, E. Lazzaro¹, M. Leigheb, G. Maddaluno, G. Maffia, M. Marinucci, D. Marocco, M. Mattioli⁴, G. Mazzitelli, C. Mazzotta, F. Mirizzi, G. Monari, S. Nowak¹, F. Orsitto, D. Pacella, L. Panaccione, M. Panella, P. Papitto, V. Pericoli-Ridolfini, L. Pieroni, S. Podda, M. E. Puiatti², G. Ravera, G. Regnoli, G.B. Righetti, F. Romanelli, M. Romanelli, F. Santini, M. Sassi, A. Saviliev⁵, P. Scarin², A. Simonetto¹, P. Smeulders, E. Sternini, C. Sozzi¹, N. Tartoni, B. Tilia, A. A. Tuccillo, O. Tudisco, M. Valisa², V. Vershkov⁶, V. Vitale, G. Vlad, F. Zonca.

Associazione Euratom-ENEA sulla Fusione
C.R. Frascati, 00044, Frascati, Roma, Italy
e-mail contact of main author: gormezano@frascati.enea.it¹

Abstract. An overview of the FTU results during the period 2003-2004 is presented. A prototype ITER-relevant LHCD launcher: the Passive Active Multijunction (PAM) has been successfully tested ($f=8\text{GHz}$). High power handling, good coupling properties and current drive effects comparable to those of a conventional launcher have been achieved. The 140 GHz ECRH system has reached its nominal performances: 1.5MW. Effective electron and ion heating (via collisions) have been observed as well as current drive (25 kA at $n_{e0}=8\times 10^{19}\text{m}^{-3}$). Avoidance and/or suppression of disruptions have been studied with ECRH. IBW studies have shown the importance of recycling in achieving improved confinement plasmas. Results achieved with advanced tokamak (AT) scenarios are presented including repetitive Pellet Enhanced Plasmas (PEP) and electron ITBs. Very peaked density profiles have been achieved with a low speed vertical pellet injector located at about mid-radius on the high field side. Performances are comparable to those achieved with a high-speed horizontal pellet injector. Possible reasons for this behaviour are discussed, among them the presence of an “MHD” drift once particles reach the $q=1$ surface. Electron ITBs can be produced at high density in FTU with LHCD. Best performances are achieved with the combined use of LHCD and ECRH. Ions are heated by collisions with $\Delta T_i/T_i$ up to 40%. A detailed analysis has shown that the ion confinement is comparable to the energy confinement time and that the ITB are not degraded by the electron-ion collisions. A database of the H_{97} factor has been established with H_{97} up to 1.6 for the e-ITBs. The peaked density profiles achieved with pellet fuelling allows the linear dependence of τ_E with n_e to be recovered. Particle pinch studies have been made at high densities in full current drive conditions where the Ware pinch plays no role. An anomalous inward pinch exists even at these high densities ($n_{e0}=1.3\times 10^{20}\text{m}^{-3}$). Parametric dependences of the density peaking are given. MHD spectroscopy has revealed high frequency modes (30-80 kHz) in the absence of energetic particles that might have consequences for burning plasmas.

1. Introduction

Experiments on the Frascati Tokamak FTU, which is a compact high magnetic field device ($R=0.93\text{m}$, $a=0.3\text{m}$, B_t up to 8T, I_p up to 1.6 MA) are aimed at developing advanced scenarios at field and densities relevant to ITER operation as well as its supporting physics [1]. The heating and current drive systems, Lower Hybrid Current Drive (LHCD, $f=8\text{GHz}$), Electron Cyclotron

¹ Associazione EURATOM-ENEA-CNR sulla Fusione, Istituto di Fisica del Plasma, Milano, Italy

² Consorzio RFX, Corso Stati Uniti 4, I-35100, Padova, Italy

³ Association EURATOM-CEA, Cadarache, F-13108, Saint Paul-lez-Durance, France

⁴ ENEA guest

⁵ A.F. Ioffe Physico-Technical Institute RAS, Polytechnicheskaya 26, 194021 St. Petersburg, Russian Federation

⁶ Nuclear Fusion Institute, RRC Kurchatov Institute, 123182 Kurchatov Sq.1, Moscow, Russian Federation

Resonance Frequency (ECRF, $f=140$ GHz) and Ion Bernstein Waves (IBW, $f=433$ MHz), are mainly interacting with electrons. Ion heating is produced by electron-ion collisions as it will be in ITER. The advanced scenarios include peaked electron temperature plasmas (electron Internal Transport Barriers: e-ITBs) or peaked electron density plasmas achieved with pellet injection (Pellet Enhanced Plasmas: PEPs).

The new hardware installed since IAEA 2002 [2] include: a high field side pellet injector, a prototype LHCD launcher for ITER and the completion of the ECRH system to 4 gyrotrons. New diagnostics include an upgrade of turbulence measurements and the installation of Fast Electrons Bremsstrahlung (FEB) cameras and a CO₂ multi-channel interferometer. Turbulence measurements on FTU are carried out using a two-channel poloidal correlation reflectometer [3//4/ which can work either in O-mode, for low-density plasmas, or in X-mode, for high density ones. This technique is systematically applied to advanced scenarios regimes when plasma conditions are such that the waves can be reflected in plasma areas of interest. Two FEB cameras (one vertical, one horizontal) detect the hard X-ray emission emitted by the fast electron tails generated by LH waves in the energy range 20 to 200keV along several chords in the poloidal cross section. This provides information on the location of these fast electrons, therefore on the localisation of LHCD allowing comparison and benchmarking with LH deposition codes to be made. The new interferometer is based on an innovative “scanning beam” technique [5/]: two CO₂ beams are spatially swept at high frequency across the plasma cross section. In this way, the density is measured along 30 chords separated in time, reconstructing one density profile every $\approx 50\mu s$.

In this paper, the main new results from the FTU heating and current drive systems will be presented first. New features of advanced tokamak scenarios including e-ITBs and PEP modes with the vertical pellet injector will be then discussed. Finally, the issues of ITER supporting physics (transport studies including particle pinch results and MHD spectroscopy) will be summarised.

2. Heating and Current Drive Systems

2.1 Lower Hybrid Current Drive. The design of the launcher mouth for ITER is very challenging: namely operation in the full shadow of the vessel port to avoid damage from escaping particle flow, withstanding of the heating due to escaping particles, radiation and neutron fluxes and achievement of high level of power handling and current drive efficiency. It has been proposed to insert one passive waveguide between each active waveguide, the so-called passive active multijunction (PAM) [6/ in order to provide for the cooling of the launcher mouth. The passive waveguides have a depth of about a quarter wavelength and reflect the wave so as to construct the required N// spectrum, although with a slightly reduced directivity than a conventional launcher. A clear conceptual advantage is to operate with very low density at the grill mouth. A prototype PAM unit (see Fig2.1) has been successfully tested in FTU [7/. An equivalent power density about 1.5 times higher than the value corresponding to the ITER request (ITER design value: 33 MW/m^2) has been launched for as long as the power can be applied (0.9s). A very low power reflection coefficient (around 1.5%) has been measured with the density in front of the launcher close to the cut-off value even with the grill mouth retracted 2 mm inside the port shadow [8/.

The fast electron tail behaviour and the overall CD efficiency have been compared with a conventional grill launching quite a similar N_{||} spectrum. Based on the FEB and loop voltage

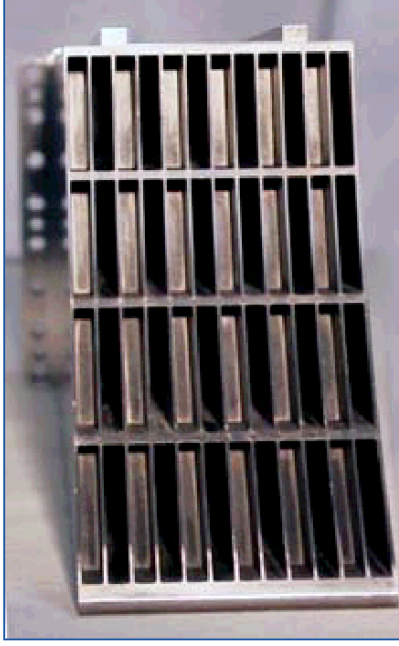


Fig2.1: View of the Passive active multijunction (PAM)

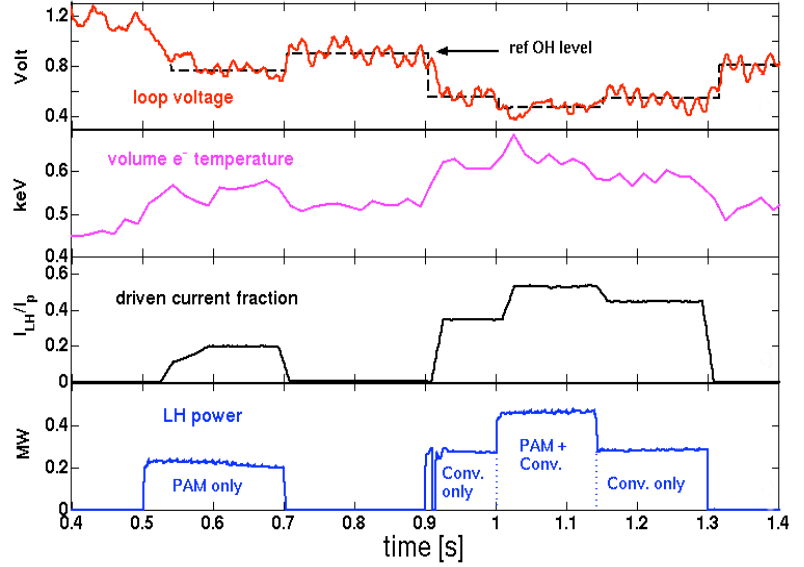


Fig.2.2: Current drive performances of the PAM antenna compared with those of a conventional grill (CG) in #24350.

data, the CD efficiencies appear to be quite similar (Fig2.2) /9/. LHCD simulation codes are carried out using the FRTC ray tracing LHCD model (1-D ($v_{||}$) Fokker Planck package) combined with the ASTRA code, that has been already benchmarked on FTU experimental data /10/. In the Fokker Planck model, ad hoc corrections to the collision operator account for 2-D effects, such as pitch angle scattering, have modelled reasonably well the FTU data. The FEB spectra obtained during a combination of the PAM and of a conventional grill are well reproduced by the modelling as shown in Fig.2.3. This LHCD modelling code, that has also been benchmarked on JET data, has been used for ITER modelling /11/ both to reassess the LHCD frequency and to predict the LHCD efficiency (Fig2.4) in the frame of an international effort /12/.

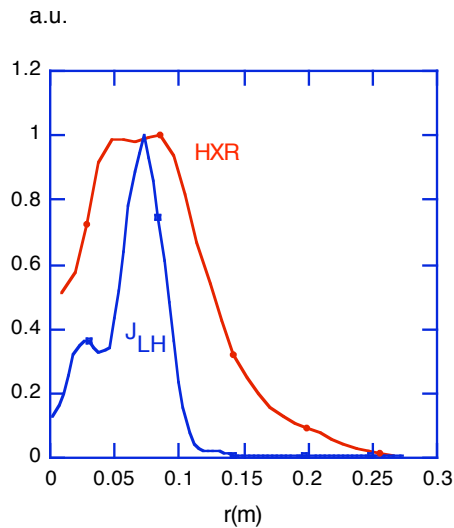


Fig2.3: Comparison of experimental FEB data for the PAM +CG phase of Fig.2.2 (HXR) with prediction from FRTC code

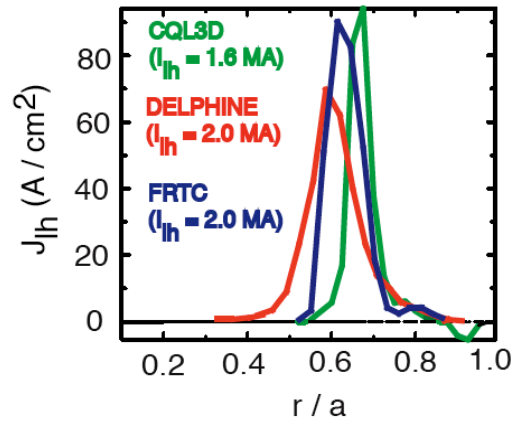


Fig2.4: Predictions of LH current density in ITER ($Q=5$ steady state scenario, $f=5$ GHz, $P_{LH}=30$ MW) using the 1-D fast ray tracing code FRTC. As a comparison, are also plotted simulations from the combined ray tracing and 2-D Fokker-Planck models CQL3D, which include trapped particle effects, and DELPHINE/13/.

2.2. Electron Cyclotron Resonance Heating

The ECRF system of FTU is progressing to reach its nominal power level of up to 1.6MW, 0.5s with four 140GHz microwave beam each focussed by an independent mirror in a 4 cm spot, with a total maximum power density of 60 MWm^{-3} . In previous experiments /1/, ECRH has been used for a large variety of applications: control of the power deposition profile allowing a large variety of energy and particle transport experiments to be studied (MHD control, synergy with LHCD fast electrons) in conditions directly relevant to ITER ($B_t = 5.3\text{T}$, $n_e = 1 \times 10^{20} \text{ m}^{-3}$). Ion heating through collisions from electrons was already observed at a power level of 0.8 MW /14/. In a first demonstrative short pulse (80ms), a dense plasma ($\langle n_e \rangle = 1.1 \times 10^{20} \text{ m}^{-3}$) has been heated with 1.5MW of ECRF power. T_{e0} increases from 1.3 to 4 keV and T_{i0} from 1.1 to 1.32 keV. Consequently the neutron yield was increased by a factor 3. ECCD experiments have been performed at a power level of $P_{EC} = 1.1 \text{ MW}$ for 400 ms. In order to have a complete first-pass absorption, plasma parameters were selected to be: $0.5 < \bar{n}_e < 0.6 \times 10^{20} \text{ m}^{-3}$ and $3 < T_e < 5 \text{ keV}$. The power density of $30\text{-}40 \text{ MW/m}^3$ leads to $0.09 < E_{||}/E_{cr} < 0.25$ (E_{cr} being the electric field above which thermal electrons can runaway/15/) and therefore a linearized theoretical treatment is adequate. A series of experiments with a toroidal injection angle set at $\pm 10^\circ$, $\pm 20^\circ$, $\pm 30^\circ$ (off perpendicular) have permitted to have a first assessment of the driven current in discharges with $I_p = 400\text{kA}$ and $2.5 < Z_{eff} < 3$. The EC driven current is estimated through plasma resistance: $I_{ECCD} = I_p - V_{loop}/R_p - I_{bs}$, with I_{bs} about 2-3% of I_p . A co-current of 15 to 25 kA has been estimated to be driven, slightly above the linear theory

The observation that in FTU ohmic discharges a drop of plasma resistivity (and in turn of toroidal electric field) due to ECRH heating produces runaway suppression during the plasma current plateau /16/ has prompted the testing of a such a scheme in disruptions. An experiment has been carried out in the 2004 campaign in which controlled disruptions ($I_p = 500\text{kA}$, $B_t = 5.3\text{T}$) have been triggered by injection of impurities (typically Mo) through laser blow-off (LBO). ECRH pulses of 20-100 ms duration have been started within few ms before the time of the disruption. Two levels of ECRH power have been used: 0.37 MW and 0.65 MW. The preliminary results indicate that ECRH power as low as 35% of the ohmic power produces a softening of the plasma current decay (i.e. longer decay) and, in several cases, even prevents the disruption when ECRH application is early enough with respect to the disruption time (see Fig.2.5). Low or no γ -ray peaks due to disruption-generated runaways are observed at an ECRH power level of 0.65 MW.

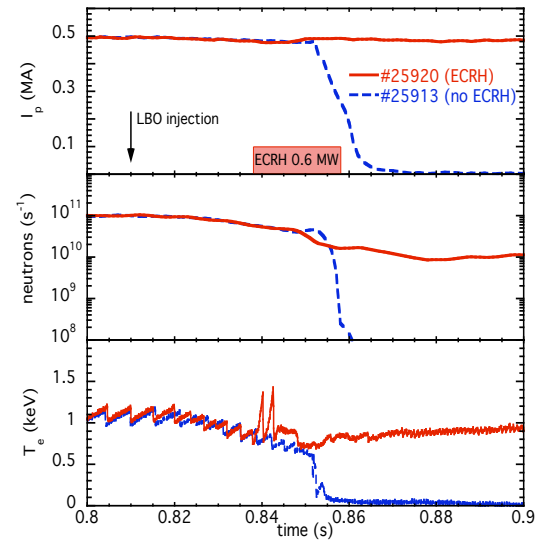


Fig.2.5: Disruptions produced by injection of Mo through LBO: effect of the application of ECRH on plasma current, neutrons and T_e

2.3. Ion Bernstein Waves. As reported in /1/, 0.4 MW of IBW power was coupled in deuterium plasma at $I_p = 0.8 \text{ MA}$, $n_e = 0.5 \times 10^{20} \text{ m}^{-3}$ and $B_t = 7.9 \text{ T}$. Some peaking of the electron pressure profile (20%) was found accompanied by a decrease of the electron thermal conductivity by 40% over the radial region inside the expected IBW deposition layer /17/. Successive experiments in 2003 were done in similar conditions. However, a higher impurity content (Mo,

O) and a higher recycling (D_α being a factor two higher) were observed. As a result, no pressure peaking with IBW power was observed, possibly due to a spurious absorption of the wave in the scrape-off plasma. Further experiments should be performed in cleaner plasmas with lower recycling in order to fully assess the role of the IBW power injection in producing confinement improvement. However, turbulence measurements were performed showing that some reduction of the turbulence level (about 20%) at the edge occurs during IBW injection /18/. O-mode reflectometry measurements on such discharges have shown some interesting behaviour. Two sets of discharges have been compared, with and without IBW, showing that inside the absorption layer the quasi-coherent (QC) component of the turbulence is reduced while the self-correlation time of the turbulence increases (but not the self correlation length). A reduction of the poloidal speed for the quasi-coherent component is also observed but not for the low frequency one. Instead, a reduction of the low frequency component is observed at about the absorption layer. The $k_\theta \rho_i$ of the QC modes is compatible with ITG turbulence. Reflectometry measurements have been carried out so far only for a set of discharges in which the improved confinement could not be reproduced.

3. Advanced Tokamak Scenarios

3.1 Improved performance plasmas with pellet injection. High-density plasmas with peaked density profiles have been achieved in FTU with multiple pellet injection /19/ from a high-speed horizontal pellet injector (2km/s). Transient improved core confinement plasmas with very low Z_{eff} has lead to record neutron yield value in FTU. Achievement of repetitive PEP modes (up to 5 subsequent pellets separated by about 100ms, 5 pellets being the maximum number of pellets available from the launcher, has permitted to maintain an average neutron yield above the ohmic values for the full duration of the current plateau (by about a factor of 2-3). A large central density peaking was observed although pellets were fully ablated at about mid-radius. Detailed analysis of the data /20/ has shown that pellet ablation near the $q = 1$ surface triggers fast growth of an $m = 1$ magnetic island: as the island reaches a large amplitude, magnetic reconnection mixes the plasma centre with the $q=1$ pellet fuelled region, so enhancing the effective pellet deposition depth. This phenomena was well reproduced by MHD codes /21/ but difficult to assess due to the geometry of the pellet launcher.

A new vertical pellet launcher has been installed to feed a vertical injection line displaced towards the high toroidal field side at a radius of $r/a \sim 0.6$. Pellets have been injected along a bent guide system (3m radius) with velocities up to 0.5km/s. As shown in Fig3.1, multiple PEP modes were achieved with performances similar to the multiple PEP modes achieved with the horizontal launcher in spite of the large distance between the tangential line and the plasma center: reheat of the electrons to the pre-pellet level and comparable increase of neutron yield. A first phase, for about 0.3-0.4ms, follows the ablation of the pellet where the ablated particles reach the $q=1$ surface. The presence of an electric radial drift due to $\nabla B/B$ is not clear and is discussed in /22/. In the second phase (from ~ 0.4 to 8 ms), an island is formed and particles drift rapidly towards the plasma center. The density profile evolve from a hollow profile to a peaked profile with the central density reaching $7-8 \times 10^{20} \text{ m}^{-3}$. This peaking is slowly increasing for the full duration of the PEP mode: here ~ 70 ms, about one τ_E . The internal mini-collapse of the PEP phase is caused by an MHD event, mainly an $m=1$ mode.

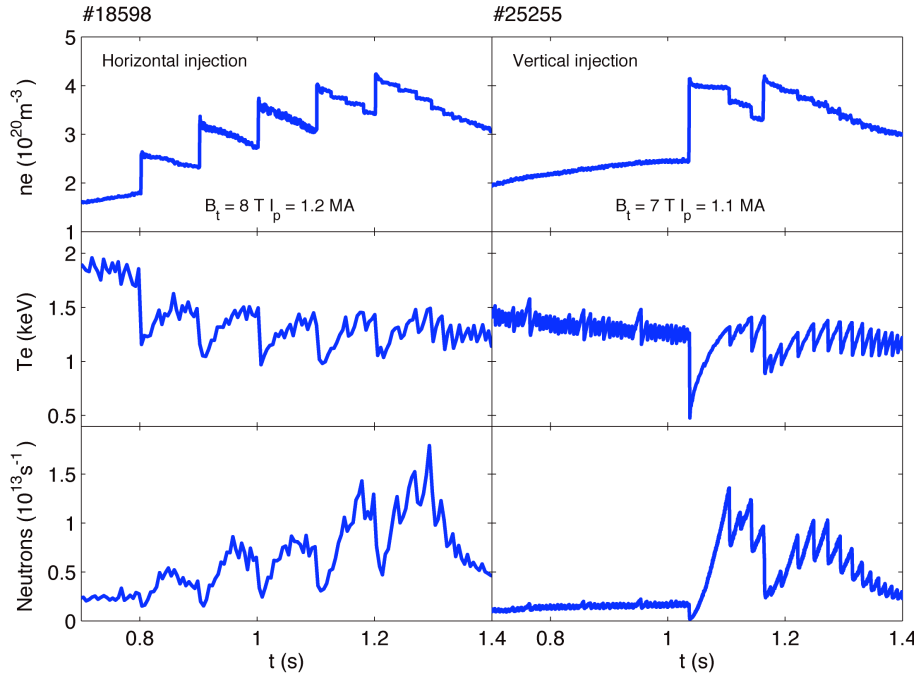


Fig3.1
Comparison of multiple PEP modes achieved with the horizontal (#18598) and the vertical (#25255)

Sometimes, an $m=2$ mode is triggered after the mini-collapse of the PEP, preventing the formation of a subsequent PEP and sometimes leading to a disruption. It has been shown that this is caused by an excessive amount of light impurities (oxygen) leading to a change of the current profile. Clean machine conditions permit to avoid this effect. Such an effect is illustrated in Fig.3.3 where the first pellet produces a PEP mode, followed by an $m=2$ mode. The turbulence is analysed by the reflectometer working in X-mode with a cut-off density of about $2.5 \times 10^{20} \text{ m}^{-3}$, so it is assumed that a cut-off layer is present in the plasma for central line average densities above $1.2 \times 10^{20} \text{ m}^{-3}$. The first pellet brings a sharp reduction in the quasi-coherent

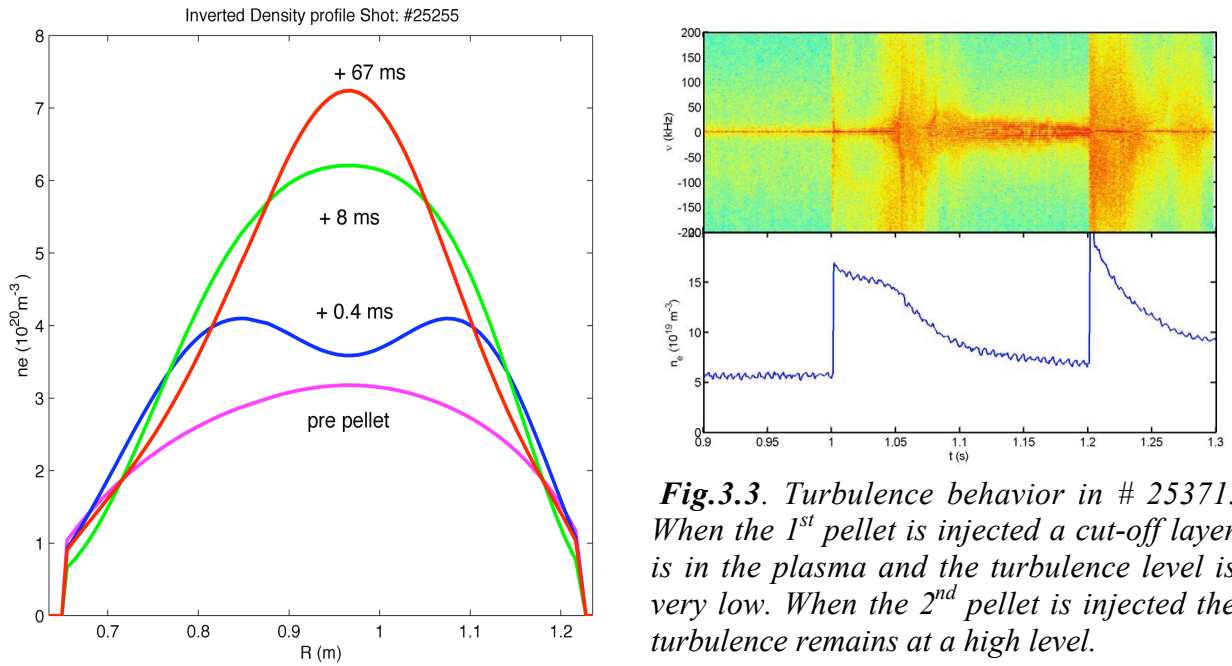


Fig.3.3. Turbulence behavior in # 25371. When the 1st pellet is injected a cut-off layer is in the plasma and the turbulence level is very low. When the 2nd pellet is injected the turbulence remains at a high level.

Fig3.2: Density peaking following vertical pellet injection (from the CO2 multi-channel interferometer). Times refer to the start of pellet injection. Particle pinch is estimated to take place around $t=0.4\text{ms}$. Error bars (about 8%) are larger when the density profile is hollow.

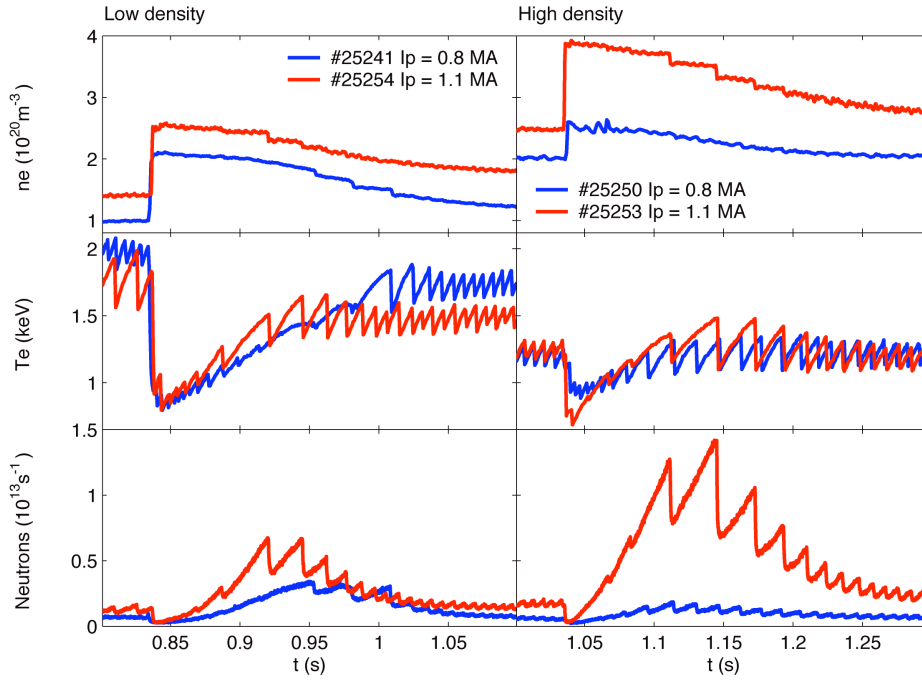


Fig3.4: Comparison of PEP modes achieved at 0.8 and 1.1 MA for which the inversion radius is $r/a \sim 0.27$ and 0.37 respectively. The vertical axis of the vertical pellet launcher is $r/a = 0.65$. At higher density, a PEP mode is not produced at 0.8 MA

component of the fluctuation spectrum. After the second pellet this reduction is not observed. The low level of turbulence corresponds to a much higher particle confinement time [23].

Some systematic studies have been done to evidence the role of the initial drift by comparing 0.8 and 1.1 MA PEPs at 7.2 T in order to increase the distance between the injection of the vertical pellet and the $q=1$ magnetic surface. A comparison between the corresponding PEPs at two different starting densities is shown in Fig 3.4. At 1.1 MA, PEPs are robust and are produced in a large range of plasma conditions. At 0.8 MA, PEPs are not produced when the target temperature is too low, likely to be due to an ineffective ablation. This increased evidence of the “MHD” pinch might alleviate some of the constraints of pellet fuelling in devices such as ITER since ablation has only to take place at a reasonable distance from the $q=1$ magnetic surface in order to fuel the plasma center.

3.2. Electron Internal Transport Barriers. Improved confinement plasmas have been achieved in the current ramp up phase ($B_t=7.0$ T, $I_p=0.8$ MA, $P_{LHCD} \approx 0.7$ MW) with LHCD only, leading to 8 keV electron temperature plasmas at densities in the range of $6 \times 10^{19} \text{ m}^{-3}$ as shown in Fig 3.5 [24]. Comparison of electron heat conductivities between an improved confinement discharge and a similar discharge without LHCD shows that central values of χ_e are reduced by more than an order of magnitude. In order to benefit from the improved LHCD efficiency at this high magnetic field, improved coupling techniques have to be developed to maintain the ITB during the plateau phase.

Improved confinement plasmas at ITER relevant parameters ($B_t=5.3$ T, $n_e \approx 10^{20} \text{ m}^{-3}$) have been achieved with combined LHCD and ECRF in magnetic configurations with a flat or mild negative shear, similar to the one corresponding to advanced scenarios for ITER: electron temperature in excess of 6 keV together with central densities in the range of $1 \times 10^{20} \text{ m}^{-3}$, H_{97} factors up to 1.6 [25]. The achieved temperature gradients correspond to electron ITBs. Recent analysis [26][27] have focused on the ion transport in these discharges where a 40% increase in ion temperature and the associated substantial increase of neutron yield (Fig. 3.6) are achieved. The neutron yield increases several times as compared to a similar discharge without ITB. Ions

are heated via collisional power transfer from electrons. However, central ion temperatures T_{i0} ($1.2 < T_{i0} < 1.6$ keV and $\Delta T_{i0} \approx 0.4$ keV) are usually smaller than T_{e0} ($3 < T_{e0} < 10$ keV and $\Delta T_{e0} \approx 7$ keV). As compared to a case without ITB, the ion conductivity is reduced all over the plasma volume down to neoclassical levels ($\chi_i \approx 0.1 \text{ m}^2 \text{ s}^{-1}$). Global ion behaviour is inferred by comparing the ion thermal energy density and the power transferred to ions by collisions with electrons in the volume inside the ITB radius. The observed relationship between these two quantities is linear and is a good indication that ions are efficiently heated from direct collisional heating. The corresponding incremental ion energy confinement time in the plasma core, $\tau_{E,i,incr} \approx 24.6$ ms, is comparable or larger than the global energy confinement time, on average 20 ms for the selected set of data /25/. However, the ratio between thermal equipartition time and energy confinement time remains at about a factor 8. Therefore, although this is a first indication that ion-electron collisions do not prevent electron ITBs to be achieved, a clear demonstration of this point would require operation at higher density and/or with higher energy confinement.

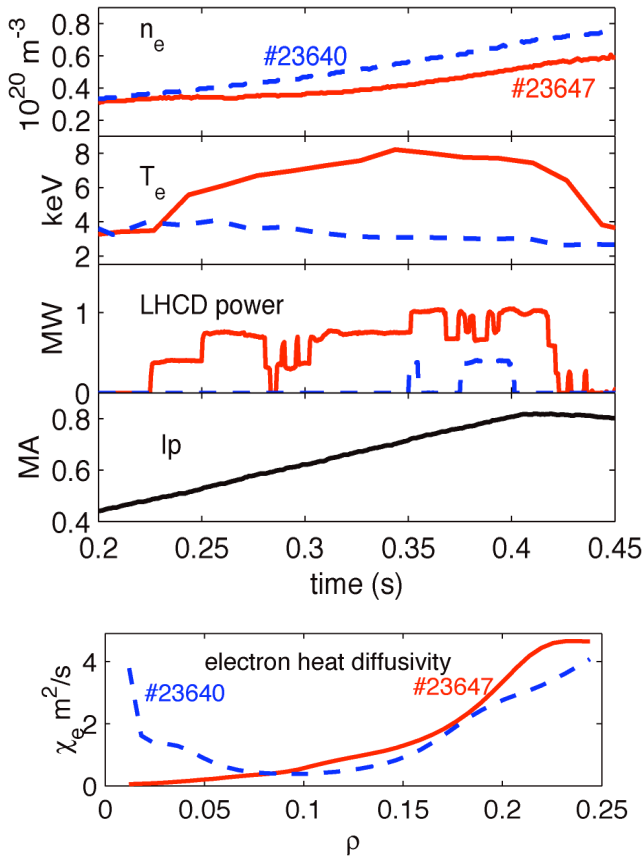


Fig3.5: Main signals of an improved confinement discharge (#23647 at $B_t=7$ T, solid line) compared with a similar discharge without LHCD (#23640, dotted line). Comparison of the respective χ_e (at $t=0.4$ s) shows an improved confinement. The LHCD power was not maintained due to coupling problems in the transition from ramp-up to plateau phase.

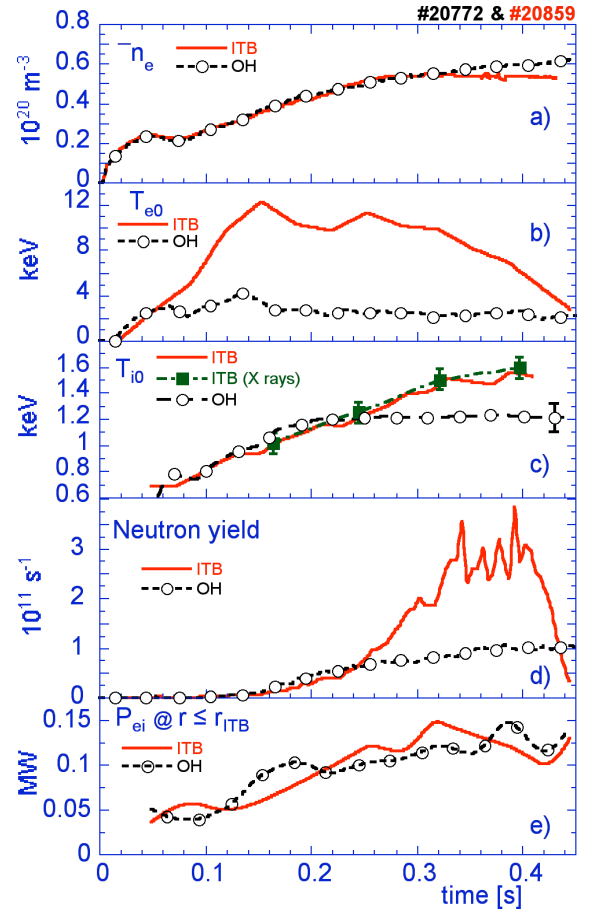


Fig 3.6: Comparison between discharges with (#20859) and without (#20772) electron ITBs. The power transferred from electrons to ions inside the ITB radius is calculated from JETTO codes calculations. 1.8 MW of LHCD was applied from $t=0.2$ s and 0.6 MW of ECRH from $t=0.07$ s to 0.28 s.

4. Supporting Physics

4.1 Heat transport analysis. A study of the confinement properties of FTU plasmas including advanced scenarios (i.e. multiple pellet fuelled, ITBs and RI modes) discharges has been carried out by means of transport code analysis and the obtained energy confinement times have been compared with the predictions of the ITER97 L-mode scaling. In the analysis, electron transport is determined experimentally from energy balance, while ion transport is based on a neoclassical model. The measured τ_E in ohmic discharges is found to be $\sim 0.92 \times \tau_{E \text{ ITER97}}$ and the linear trend with the line-averaged density saturates at a value of ~ 50 ms for $\bar{n}_e > 0.5 \times \bar{n}_{\text{Greenwald}}$. Standard L-mode (with ECRH, IBW and LH additional heating) as well as RI mode discharges are in good agreement with the ITER97 L-mode scaling predictions. An improvement of τ_E up to 60% with respect to the ITER97 L-mode scaling is found for additionally heated discharges (LH plus ECRH or LH only) in which ITB formation has occurred.

Transport analysis of a set of 7.2 T ohmic discharges was performed with the JETTO code in order to investigate the effect of pellet injection on the energy confinement time (τ_E) /28/. The results are shown in Fig.4.1 where data for both pellet and gas fuelled discharges are plotted. The linear phase of τ_E versus the line-integrated density (\bar{n}_e) can be described as:

$$\tau_E^{\text{linear}} (\text{ms}) = k \bar{n}_e q^{1.42 \pm 0.07}$$

(\bar{n}_e is in 10^{20} m^{-3} units, q is the cylindrical safety factor and k is a constant). The peaked density profiles obtained by pellet fuelling allow the linear dependence of τ_E on \bar{n}_e to be recovered at high-density regimes at high current. The saturation of τ_E with increasing density can be related to the change (at high density) from electron to ion transport dominated regime. The improvement of confinement with pellet corresponds to a strongly reduced χ_i as compared with the χ_i in the gas-fuelled case at the same density: this is in qualitative agreement with theory

/29/ which predicts the suppression of ion temperature gradient modes with density peaking.

4.2 Particle pinch. Particle transport will have a large impact on the density profile in ITER, where central fuelling will be negligible, in influencing the density profile and consequently the overall confinement. The particle flux, including turbulent transport /30//31/, can be written as:

$$\Gamma = -D [\nabla n + C_q \nabla q / q n - C_T \nabla T_e / T_e n] + V_{\text{Ware}} n$$

where D is a turbulent diffusion coefficient. The so-called Ware pinch, or neo-classical pinch, is mainly driven by the toroidal electric field. It is therefore of particular interest to assess such a pinch effect in experiments with full non-inductive current drive leading to a null toroidal

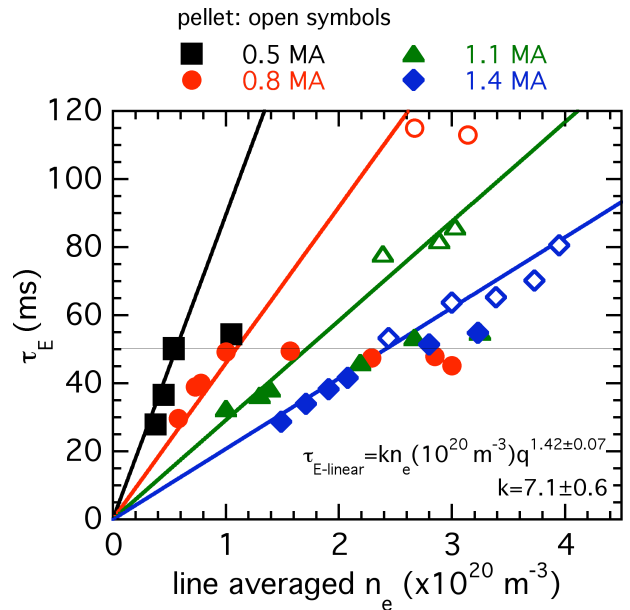


Fig.6.1: Effect of pellets (open symbols) on energy confinement time: the linear (neo-Alcator) scaling with density is recovered in multiple-pellet fuelled discharges (pellet τ_E data are averaged over 50 ms). The horizontal line represents the saturation ohmic confinement time in FTU.

electric field with only RF heating and current drive techniques without any internal fuelling.

The existence of an anomalous inward pinch in steady state plasma without electric field was demonstrated in Tore Supra /32/. However, such a demonstration was done at rather low density: $n_e(0)=2-3.5 \times 10^{19} \text{ m}^{-3}$ and $T_e(0)=4.8 \text{ keV}$. A similar set of experiments has been done in FTU in conditions of higher density and collisionality more relevant to ITER. Full current drive conditions were achieved with 1.6MW of LHCD for the following conditions /1/: $B_t=7.2 \text{ T}$, $I_p=0.5 \text{ MA}$, $n_{e0}=1.3 \times 10^{20} \text{ m}^{-3}$ and $T_{e0}=6 \text{ keV}$ for about $3\tau_E$, followed by almost full current drive ($\Delta V_{\text{loop}}/V_{\text{loop}}=90\%$ with $V_{\text{loop}}=0.1 \text{ V}$) for a further $10\tau_E$. The normalised density profile flattens significantly during the full current drive phase, as shown in Fig 4.2, but remains peaked. The profile remains unchanged during the full duration of the quasi full current drive phase.

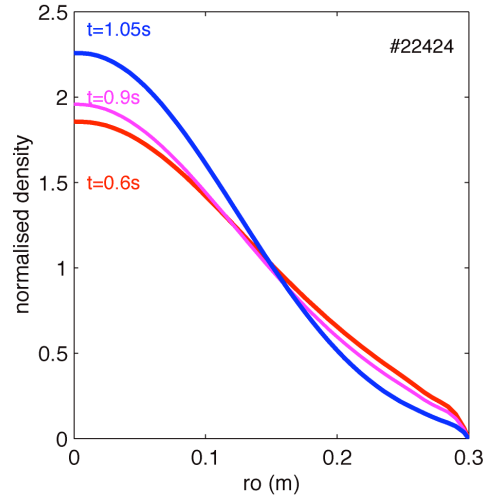


Fig6.2: normalised density profiles without LHCD($t=1.05\text{s}$), with full current drive ($t=0.6\text{s}$) and with almost full CD($t=0.9\text{s}$, $\Delta V/V=90\%$)

Data analysis /23/ confirms the results found in Tore Supra at a lower collisionality: the scaling of the density peaking with the temperature gradient depends upon the area of the plasma with a transition phase at about $r/a=0.3$ (Fig 4.3). Density peaking depends also almost linearly with $\nabla q/q$ (Fig 4.4). Attempts to understand these results and to assess their consequence for ITER are underway.

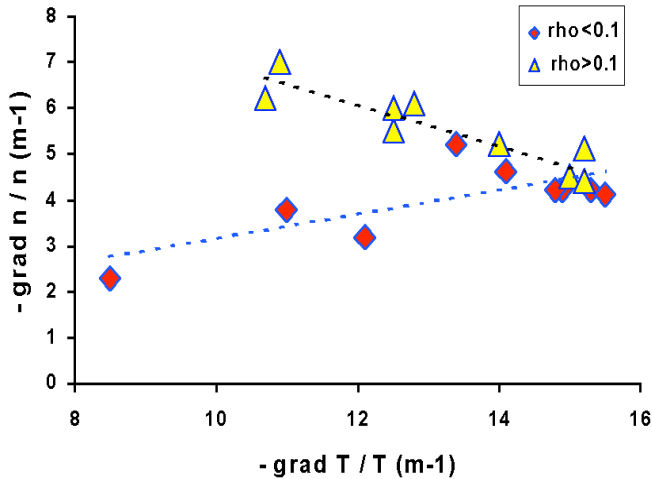


Fig 6.3: Dependence of $\text{grad } n/n$ with $\nabla T/T$ (#22424 and #21638)

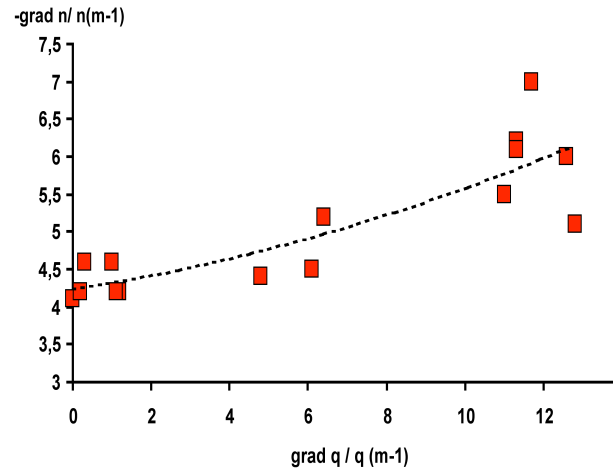


Fig 6.4: Dependence of $\nabla n/n$ with $\nabla q/q$ (#22424 and #21638)

4.3 MHD spectroscopy has revealed high frequency (HF) oscillations that accompany the development of $m=2$, $n=1$ islands [33]. The threshold corresponds to an $m=2$ poloidal field relative perturbation of 0.2%. A typical spectrogram of these HF oscillations is shown in Fig.4.5. Frequency of these modes is almost 70 kHz, which is inside the low frequency gap introduced in the Alfvénic spectrum by finite beta effects, while the first toroidal gap is one order of magnitude higher. Since in these ohmic plasmas there are no fast ions that can excite Alfvén modes, the observed perturbations are likely to be due to the non-linear excitation of shear-Alfvén waves by the magnetic island. The interaction between these waves and fast particles in burning plasma could be a new loss mechanism that develops below the threshold for energetic particle modes excitation.

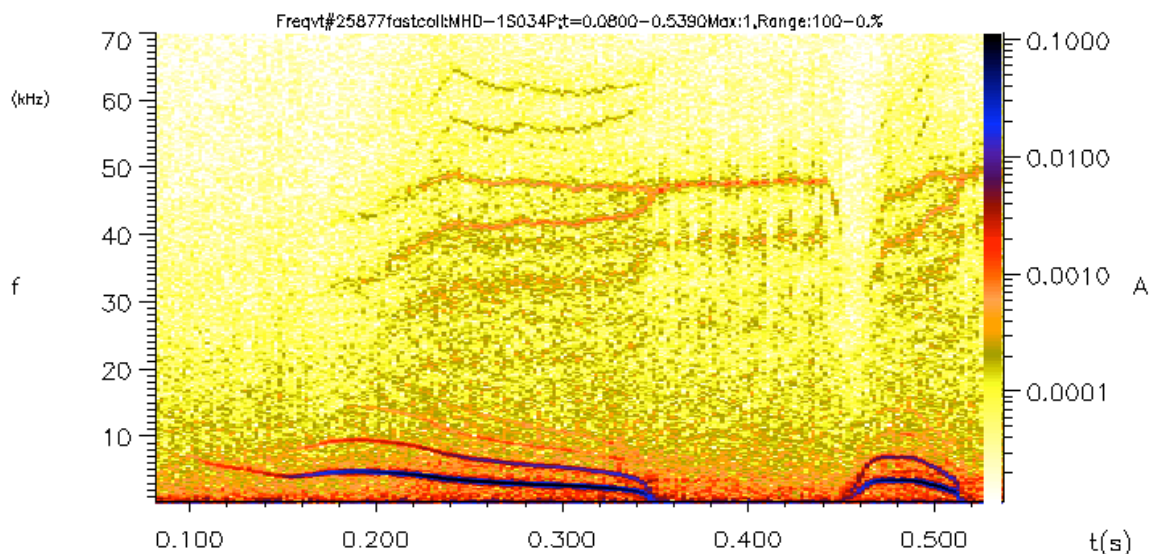


Fig.4.5 Spectrogram of a Mirnov coil for #25877. Ordinates and color scales indicate frequency and amplitude respectively. Intense lines below 20 kHz correspond to a (2,1) tearing modes and its harmonics while lines above 30 kHz correspond to the high frequency waves.

5 Perspectives

FTU will resume operation in 2005 with the exploitation of the LHCD, the ECRH, the IBW systems at their full power capability. Active control of MHD (tearing modes) with ECRH is being prepared. A more systematic study of disruption mitigation will be done by triggering the EC power at the time of the change of V_{loop} associated with the start of the disruption. It is also planned to install an active beam diagnostic system with the aim of measuring ion temperature profiles and also the current profile through motional Stark effects (MSE). It is also planned to install a lithium limiter, in collaboration with the TRINITY Institute (Russia), where the lithium diffuses through capillarity allowing different conditioning techniques (boronisation, titanisation,...) to be compared. Assessment of the capability of such a capillary system to withstand the electromagnetic forces in a tokamak, therefore avoiding pollution from lithium droplets, will be attempted.

References

- /1/ Special Issue on FTU in *Fusion Science and Technology* (Guest editor C.Gormezano) **45** (May 2004);
- /2/ Angelini. B., *et al*, *Nucl. Fusion* **43** (2003) 1632-1640;
- /3/ Vershkov V.A., Dreval V.V., Soldatov S.V., *Rev. Sci. Instr.*, **70** (1999);
- /4/ Vershkov V.A., *et al*., 28th *EPS Conf. on Plasma Physics, Madeira (2001)*, P1.011;
- /5/ Tudisco O., *et al*, *Fusion Science & Tech.* **45** (2004) 402;
- /6/ Bibet Ph., *et al*, Rep. EUR-CEA-FC-1520, CEN Cadarache, France, Sept. 1994;
- /7/ Mirizzi F., *et al*, 20th *Symposium on Fusion Engineering (SOFE 2003)*, Oct.2003, San Diego, USA;
- /8/ Pericoli Ridolfini V., *et al*, 31st *EPS Conf. on Plasma Physics (London, 28th June-2nd July 2004)* P2-105;
- /9/ Pericoli Ridolfini V., *et al*, this conference, EX/5-5;
- /10/ Barbato E., *et al*, *Fusion Science & Tech.* **45** (2004) 323;
- /11/ Barbato E., Saviliev A., 31st *EPS Conf. on Plasma Physics (London, 28th June-2nd July 2004)* P2-104;
- /12/ within the ITPA Topical Group on Steady State Operation: being prepared for the Tokamak Physics Basis (to be submitted to Nuclear Fusion);
- /13/ Bonoli P., *et al*, in *Radio Frequency power in Plasmas*, AIP Conf. Proc. 694, Ed. C.B. Forest, (AIP,NY,2003)24;
- /14/ Granucci G., *et al*, *Fusion Science & Tech.* **45** (2004) 387;
- /15/James R.A., Giruzzi G., *et al*, *Phys. Review A*, **45** (1992) 8783;
- /16/ J.R. Martin-Solis, *et al*., *Nucl. Fusion*, **44** (2004) 974;
- /17/ Castaldo C., *et al*. *Nucl. Fusion* **44**, (2004) L1-L4;
- /18/ De Benedetti M., *et al*., in proc. *Conf. on Plasma Physics (London, 28th June-2nd July 2004)*;
- /19/ Frigione D., *et al*, *Nucl. Fusion* **41** (2001) 1613;
- /20/ Giovannozzi E., *et al*, *Nucl. Fusion* **44** (2004) 226;
- /21/ Annibaldi S.V., *et al* *Nucl. Fusion* **44** (2004) 12;
- /22/ Giovannozzi E., *et al*, this conference, EX/P4-4;
- /23/ Romanelli M., *et al*, this conference, EX/P6-24;
- /24/ Castaldo C., *et al*, to be submitted to Nuclear Fusion;
- /25/ Pericoli Ridolfini V., *et al*, *Nucl. Fusion* **43** (2001) 287;
- /26/ Barbato E., Pericoli Ridolfini V., *et al*, *Fusion Science & Tech.* **45** (2004) 387;
- /27/ Gormezano C., *et al*, 30th *EPS Conf. on Plasma Physics (St Petersburg, 7-11 July 2003)* P2-145;
- /28/ Esposito B., *et al*, *Plasma Phys. Control. Fusion* **46** (2004) 1793-1804;
- /29/ Hassam A.B., *et al*. *Phys. Fluids* **B2**(8) (1990) 1822;
- /30/ Romanelli F. and Zonca F., *Phys. Fluids* **B6** (11) (1993) 4081;
- /31/ Garbet X., *et al*, *Phys. Rev. Letters* **91**(2003) 035001;
- /32/ Hoang G.T., *et al*, *Phys. Rev. Letters* **90** (2003) 155002;
- /33/ Buratti P., *et al*, this conference, EX P5-1;